JOURNAL OF BACTERIOLOGY, June 1994, p. 3303–3313
0021-9193/94/$04.00+0

Vol. 176, No. 11

Structural and Antigenic Characteristics of *Campylobacter coli* FlaA Flagellin

MARY E. POWER,[1] PATRICIA GUERRY,[2] WILLIAM D. McCUBBIN,[3] CYRIL M. KAY,[3] AND TREVOR J. TRUST[1]*

Department of Biochemistry and Microbiology, University of Victoria, Victoria, British Columbia V8W 3P6,[1] and Medical Research Council Group in Protein Structure and Function, Department of Biochemistry, University of Alberta, Edmonton, Alberta T6G 2H7,[3] Canada, and Enteric Diseases Program, Naval Medical Research Institute, Bethesda, Maryland 20814[2]

Received 7 December 1993/Accepted 21 March 1994

The polar flagellar filament of *Campylobacter coli* VC167 is composed of two highly related (98%) flagellin subunit proteins, FlaA and FlaB, whose antigenic specificities result from posttranslational modification. FlaA is the predominant flagellin species, and mutants expressing only FlaA form a full-length flagellar filament. Although the deduced M_r of type 2 (T2) FlaA is 58,884 and the apparent M_r by sodium dodecyl sulfate-polyacrylamide gel electrophoresis is 59,500, the solution weight-average M_r by sedimentation analysis was 63,000. Circular dichroism studies in the presence or absence of 0.1% sodium dodecyl sulfate or 50% trifluorethanol showed that the secondary structure of T2 FlaA flagellin was altered, with α-helix structure being increased to 25% in the nonpolar environment. The molecule also contained 35 to 48% β-sheet and 11 to 29% β-turn structure. Mimeotope analysis of octapeptides representing the sequence of FlaA together with immunoelectron microscopy and enzyme-linked immunosorbent assay with a panel of antisera indicated that many residues in presumed linear epitopes were inaccessible or nonepitopic in the assembled filament, with the majority being in the N-terminal 337 residues of the 572-residue flagellin. Residues at the carboxy-terminal end of the T2 FlaA subunit also become inaccessible upon assembly. Digestion with trypsin, chymotrypsin, and endoproteinase Glu-C revealed a protease-resistant domain with an approximate M_r of 18,700 between residues 193 and 375. Digestion with endoproteinase Arg-C and endoproteinase Lys-C allowed the mapping of a segment of surface-exposed FlaA sequence which contributes serospecificity to the VC167 T2 flagellar filament at residues between 421 and 480.

Flagella are the structures responsible for the swimming motility of numerous bacterial species. The flagella best described at both the structural and molecular levels are those of members of the enteric bacterial genera *Escherichia* and *Salmonella*. The unsheathed flagella of these organisms are formed by the polymerization of a single species of flagellin. Another group of bacteria produce unsheathed flagellar filaments composed of two or more species of flagellin. These "complex" filaments have been described for species of *Campylobacter* (11, 27), *Caulobacter* (41), and *Rhizobium* (31). The periplasmic flagella of spirochetes (28, 29) are also composed of multiple species of flagellin subunits, as are the flagellar filaments of archaea (9, 17). In several of these organisms, the flagellin genes coding for the two or more flagellin species have been sequenced. However, as a group, the complex flagella remain poorly described.

The complex polar flagellum of the diarrheal pathogen *Campylobacter coli* contains two species of flagellin, FlaA and FlaB, which are encoded by two genes that are located adjacent to one another in a tandem orientation (11, 13). In *C. coli* VC167 these flagellin genes express highly related species of flagellin protein, each containing 572 amino acid residues (12). Northern (RNA) analyses have shown that the *flaA* and *flaB* genes are expressed concomitantly in both type 1 (T1) and type 2 (T2) cells and that the mRNA for each size is unit length rather than polycistronic (13). Each gene has an independent promoter, with *flaA* being transcribed from a typical σ^{28} promoter (13), while *flaB* is transcribed from a σ^{54} promoter (11) which is susceptible to environmental regulation (2). Primer extension experiments have further shown that more *flaA* transcript than *flaB* transcript is present (13). Mutants defective in both genes are nonmotile and nonflagellated (11) and are unable to colonize the rabbit intestine (30). Mutants defective in the *flaA* gene are partially motile and produce a severely truncated filament, while mutants defective in the *flaB* gene are slightly less motile than wild-type cells and produce a flagellum indistinguishable in length from the wild type (11). Therefore, both flagellin species appear to be required for maximum motility, although FlaA is clearly the predominant species in the *Campylobacter* flagellar filament.

In the case of *C. coli* VC167, variants which produce antigenically distinct flagella, T1 and T2, have been isolated. Cells producing T2 flagella display higher motility (12) and are preferentially selected during colonization in an animal model (22). The flagellin species constituting these two antigenic types of flagella can be distinguished from each other by differences in their reaction with two different polyclonal antisera, LAH1 and LAH2 (14). In addition, the T1 flagellins display an apparent subunit M_r of 61,500 by sodium dodecyl sulfate-polyacrylamide gel electrophoresis (SDS-PAGE), while the T2 flagellins display an apparent subunit M_r of 59,500 (1). The deduced M_rs of the VC167-T1 *flaA* and *flaB* gene products are 58,916 and 58,946, respectively, while the *flaA* and *flaB* genes of VC167-T2 encode flagellins with predicted M_rs of 58,884 and 59,124, respectively (12). Recent studies in which the flagellin structural genes from a T1 background were expressed in a T2 background, and vice versa, have shown that

* Corresponding author. Mailing address: Department of Biochemistry and Microbiology, University of Victoria, Victoria, B.C. V8W 3P6, Canada. Phone: (604) 721-7079/7086. Fax: (604) 721-8855. Electronic mail address: ttrust@sol.uvic.ca.

both the electrophoretic mobility differences in SDS-PAGE and the LAH serospecificities of the flagellins are conferred by the host background and not by the primary amino acid sequence (1), indicating that the LAH serospecificities of the *C. coli* VC167 flagellins are the result of posttranslational modifications. Other studies have shown that certain serine residues are subject to posttranslational modification (24).

To provide more information on this important *Campylobacter* immunogen and motility organelle, we have examined the biochemical and immunochemical structures of the predominant FlaA protein from the biologically significant and posttranslationally modified T2 serotype flagella of *C. coli* VC167. The protein was subjected to solution molecular weight determination, to secondary structure analysis by far-UV circular dichroic spectral analysis, near-UV circular dichroic spectral analysis, proteolytic analysis of domain structure, and determination of LAH2 serospecificity, and to mimeotopic analysis of amino acid residues buried in the assembled flagellar filament. Here we report our findings.

MATERIALS AND METHODS

Bacterial strains and culture conditions. *C. coli* VC167 serogroup LIO8 was originally obtained from H. Lior, National Enteric Reference Centre, Ottawa, Ontario, Canada. *C. coli* C167-T1 and VC167-T2 are stable laboratory derivatives that produce antigenic T1 and T2 flagellar filaments, respectively (14). Mutant *C. coli* VC167-T2 KX5 (*flaA*$^+$ *flaB*), which produces a full-length FlaA filament, was constructed by insertion of a kanamycin cassette into the *flaB* gene (11). Campylobacters were grown on Mueller-Hinton agar (Difco Laboratories, Detroit, Mich.) or on Mueller-Hinton agar supplemented with kanamycin (50 μg/ml) at 37°C in a nitrogen atmosphere containing 5% oxygen and 10% CO_2.

Electrophoresis. SDS-PAGE was performed by the method of Laemmli (19), using a mini-slab gel apparatus (Hoefer Scientific Instruments, San Francisco, Calif.). Proteins were solubilized in sample buffer containing 2-mercaptoethanol and SDS, stacked in 4.5% acrylamide (100 V, constant voltage), and separated in 15 or 20% acrylamide (150 V, constant voltage). Protein was stained with Coomassie brilliant blue R250 (Sigma Chemical Co., St. Louis, Mo.). When required, the separated proteins or peptides were electrophoretically transferred to nitrocellulose paper in a Novablot apparatus (Pharmacia LKB, Bromma, Sweden) at 15 V for 36 min, using the methanol-Tris-glycine buffer system of Towbin et al. (36) for immunological detection, or to ProBlott membrane (Applied Biosystems, Foster City, Calif.), using 100 mM 3-cyclohexylamino-1-propane sulfonic acid (CAPS) buffer (pH 11) (Aldrich Chemical Co., Milwaukee, Wis.) by the method of LeGendre and Matsudaira (21). For sequence analysis, the blotted peptides were stained with Coomassie blue and cut from the membrane.

Protein purification. Intact FlaA flagellar filaments were isolated from 24-h cultures of *C. coli* VC167-T2 KX5. Cells were harvested in 10 mM Tris HCl–0.85% (wt/vol) NaCl (Tris-NaCl) (pH 7.4) and homogenized for 2 min. Whole cells and cell debris were removed by two low-speed centrifugations (10,000 × *g*, 20 min), and the resulting supernatant was subjected to ultracentrifugation (100,000 × *g*, 60 min). The pellet was resuspended in 1% (vol/vol) SDS in distilled water and subjected to ultracentrifugation as before. The SDS washing was repeated until the flagella were purified to homogeneity as determined by the presence of only flagellar filaments in negatively stained preparations examined by electron microscopy and by the presence of only the bands corresponding to T2 FlaA flagellin (apparent M_r, 59,500) (1) and hook protein (apparent M_r, 92,500) (32) bands in Coomassie blue-stained SDS-PAGE gels. The final pellet was then washed three times in distilled water and stored in distilled water until required.

FlaA flagellin was purified from the first crude sheared flagellum ultracentrifugation pellet described above. Flagella in the pellet were dissociated in 0.2 M glycine (pH 2.2) for 30 min at 4°C, and insoluble material was removed by ultracentrifugation (100,000 × *g*, 1 h). Flagellin protein in the glycine-soluble fraction was then subjected to molecular exclusion chromatography on a Superdex 75 fast protein liquid chromatography (FPLC) column (Pharmacia, Uppsala, Sweden) in 20 mM Tris buffer (pH 7.5) at a flow rate of 0.7 ml/min. Flagellin-containing fractions were pooled, and the purity of the preparation was confirmed by the presence of a single band in SDS-PAGE. The major trypsin-resistant flagellin peptide was purified by FPLC under identical conditions. When required, solvent exchange and concentration of flagellin solutions were accomplished by the use of membrane centrifugal microconcentrator devices (Filtron Technology Corporation, Northborough, Mass.).

Protein characterization. The solution molecular weight was determined by analytical ultracentrifugation. A Beckman model E analytical ultracentrifuge equipped with electronic speed control, a Rotor Temperature Indicator and Control (RTIC) temperature control system, and a titanium rotor was used for all runs. The Photoelectric Scanner Optical System was employed for measurements to determine molecular weights. Determinations of molecular weights were performed by the sedimentation equilibrium technique described by Chervenka (5). The sample (100 μl) was loaded into a 12-mm double-sector, charcoal-filled Epon cell equipped with sapphire windows. Runs were performed at 20°C for 48 h in 200 mM glycine HCl (pH 2.2) before equilibrium traces were taken. Molecular weight calculations were carried out with a computer program written in the APL language. In these calculations a value of 0.73 ml/g was assumed for the partial specific volume of the protein. The data for $\ln y$ versus r^2 data were fitted to a second-degree polynomial equation by least-squares techniques, and the point-average molecular weights were calculated from the slope of this equation.

Measurement of sample concentrations for determination of extinction coefficients was performed by using the methodology of Babul and Stellwagen (4). A 120-μl aliquot of sample was loaded in one side of a 12-mm double-sector synthetic boundary cell, and the other side was filled with solvent. The cell was installed in a rotor and centrifuged at 3,000 × *g*. As the solvent was layered onto the sample solution, the boundary created was visible as a bending of the fringes in the interference optical system. Photographs of the boundary formation were measured on the microcomparator to determine the number of fringes traversed when the boundary between the solvent and sample regions was crossed. An average refractive increment of 4.1 fringes per mg per ml was used to relate the number of fringes to concentration. Also, by using the known amount of tyrosine residues in the flagellin molecule (12), a theoretical extinction coefficient was calculated, and measurement of the absorption spectrum from 350 to 250 nm allowed a concentration to be established.

Circular dichroism (CD) measurements were made on a Jasco J-720 spectropolarimeter (Jasco Inc., Easton, Md.) interfaced to an Epson Equity 386/25 and controlled by Jasco software. The thermostat-equipped cell holder was maintained at 25°C with a Lauda RMS circulating water bath (Lauda, Westbury, N.Y.). The instrument was routinely calibrated with ammonium *d*-(+)-10 camphor sulfonate at 290.5 and 192 nm

and with *d*-(−)-pantoyllactone at 219 nm. Each sample was scanned 10 times, and noise reduction was applied to remove the high frequency before molar ellipticities were calculated. The voltage to the photomultiplier was kept below 500 V to prevent distortion of the CD spectra. Cells used for the region below 255 nm were 0.05 cm (calibrated for path length). The protein concentration used was 0.989 mg/ml by fringe counting. The equation $[\theta] = \theta_{obs}/10lc$ was applied, where θ_{obs} is in degrees (the instrument measures in millidegrees), l is path length in centimeters, and c is concentration in grams per cubic centrimeter per mean residue weight. In the calculation we used the concentration C in either milligrams per milliliter per mean residue weight or $M \times N$, where M is the molar concentration of the protein and N is the number of amino acids in the protein. The unit for molar ellipticity was degree-centimeter squared per decimole. The CD spectra were analyzed by the Contin program (version 1.0) of Provencher and Glöckner (33), which analyzes CD spectra as a sum of spectra of 16 proteins, the structures of which are known from X-ray crystallography.

For limited proteolysis with trypsin and chymotrypsin, purified flagellin or flagellar filaments were suspended in 100 mM Tris HCl containing 10 mM $CaCl_2$ (pH 7.8) and were incubated with tosylphenylalanine chloromethyl ketone (TPCK)-treated bovine pancreatic trypsin (Sigma) or chymotrypsin (Boehringer) at a protein-to-enzyme ratio of 250:1 at room temperature. At various times from 5 min to 5 h, 20-μl samples were removed, inactivated with equimolar trypsin inhibitor or phenylmethylsulfonyl fluoride, and added to an equal volume of SDS-PAGE sample buffer. The samples were immediately boiled for 5 min. Alternatively, the proteins were suspended in 50 mM phosphate buffer (pH 7.8) and incubated with endoproteinase Glu-C (staphylococcal V8 protease; Boehringer) at a protein-to-enzyme ratio of 200:1 at room temperature. Samples were taken and treated as described above. Digestions were also performed with endoproteinase Lys-C (Boehringer) at a protein-to-enzyme ratio of 100:1 in 0.1 M ammonium bicarbonate buffer (pH 8.5) at 37°C for up to 18 h. In this case digestion was stopped with excess protease inhibitor Nα-*p*-tosyl-L-lysine chloromethyl ketone (TLCK) (Boehringer). In addition, digestions were performed with endoproteinase Arg-C (Boehringer) at a protein-to-enzyme ratio of 50:1 in 0.1 M ammonium bicarbonate buffer (pH 8.2) and 1 mg of SDS per ml at 37°C for up to 9 h. This digestion was again stopped with excess protease inhibitor TLCK (Boehringer). For amino acid sequence analysis of peptides generated by limited proteolysis, peptides were submitted to SDS-PAGE and electroblotted, and the blotted Coomassie blue-stained excised bands on a ProBlott membrane were analyzed in an Applied Biosystems model 470A gas phase sequenator.

Expression of *C. coli* flagellin epitopes in *Salmonella* flagellin. Synthetic oligonucleotides specifying two epitopes of VC167 flagellins were inserted into the hypervariable region of the *Salmonella* flagellin gene in pLS408 (26, 43). Two synthetic, partially complementary oligonucleotides (PG60 [5′-TTTAA TGCATATAATGGTGGTGGTGCAAAA-3′] and PG61 [5′-TGCAAAAATAATCTGTTTTGCACCACCACC-3′]) were phosphorylated with T4 polynucleotide kinase (Boehringer), annealed, and treated with Klenow enzyme to produce a blunt-ended 45-bp molecule capable of encoding amino acid residues 370 to 393 of the *flaA* and *flaB* flagellin genes (FNAYNGGGAKQIIFA), using codons preferred in the *Salmonella dublin* flagellin gene (40). The blunt-ended molecule was cloned into pLS408 which had been digested with *Eco*RV and dephosphorylated with calf intestinal alkaline phosphatase (Boehringer). Six random clones were picked and subjected to DNA sequence analysis using a synthetic primer (PG72 [5′-GCTGTAACCGTTGATAA-3′]) located 42 bp upstream of the insertion point (40). Two clones which had a single copy of the 45-bp fragment inserted in the correct orientation were identified, and one of these, termed pGK300, was used in subsequent studies.

A similar construction was done by using two oligonucleotides (PG73 [5′-CAGATTAACTATAACGATGGTGATAA CAAC-3′] and PG74 [5′-AGAAATCAGCTGACCGTTGT TATCACCATC-3′]) capable of encoding amino acid residues 261 to 275 (QINYNDGDNNGQLIS) of the *flaB* gene (12). Four clones were subjected to DNA sequence analysis, and two were found to be in the correct orientation. One of these, pGK301, was used in subsequent studies. The two recombinant plasmids isolated from *Escherichia coli* DH5 were transferred into *S. dublin* SL5928 (*aroA148* HI-*i*::Tn*10*) by electroporation. The presence of either recombinant plasmid reduced the observed motility of SL5928 compared with that in the presence of pSL408 without the insertions.

Double-stranded dideoxy sequence analysis of clones was performed with Sequenase (U.S. BIOmedicals, Cleveland, Ohio) and custom synthetic primers purchased from Synthecell, Gaithersburg, Md.

Antibodies. All polyclonal antisera were raised in rabbits. Polyclonal antiserum LAH2 was raised against *C. coli* VC167-T2 whole cells and extensively absorbed against T1 whole cells as previously described (14). This antiserum contained antibodies which reacted with T2 flagella but not with T1 flagella. Polyclonal antiserum MEP2 was raised against formalin-killed whole cells of *C. coli* VC167-T2; polyclonal antiserum E288 was raised against *C. coli* VC167-T2 flagellin protein which had been subjected to SDS-PAGE, electroblotted to nitrocellulose, and cut from nitrocellulose to immunize the rabbit; and polyclonal antiserum M27 was raised against the high-pressure liquid chromatography (HPLC)-purified flagellin monomer. Polyclonal antiserum Y29 was raised against a fusion of *C. coli* VC167-T2 residues 55 to 335 to protein A in pRIT5 (Pharmacia, Picataway, N.J.) and absorbed extensively against protein A, while polyclonal antiserum Y30 was raised against *S. dublin* carrying flagella containing a *Salmonella* flagellin fusion expressing *C. coli* VC167-T2 FlaB residues 261 to 275. Y30 was absorbed extensively against whole cells of *S. dublin* expressing wild-type flagella. Antiserum PG4 was raised against a synthetic peptide corresponding to amino acids 170 to 180 (12) of the *C. coli* VC167-T2 flagellin coupled to bovine serum albumin (BSA).

Polyclonal antiserum LINA was raised against formalin-killed whole cells of *C. coli* VC167-T1, while polyclonal antisera SML1 and SML2 were raised against whole cells and flagellin, respectively, cut from nitrocellulose, of heterologous *C. jejuni* VC74. Monoclonal antibody M39 was also raised against *C. jejuni* VC74 flagellin, while monoclonal antibody 72c was raised against *Helicobacter pylori* flagellin (18). These polyclonal and monoclonal antibodies are cross-reactive with a variety of campylobacter and helicobacter flagellins by Western immunoblot analysis. The various antibodies and antisera used are summarized in Table 1.

Peptide synthesis and epitope scanning. The amino acid sequences of both of the *C. coli* VC167-T2 flagellins, predicted from the DNA sequences (12), were used to develop octameric peptides overlapping by four amino acids and encompassing the entire FlaA protein and the regions of difference of FlaB from FlaA. A commercially available kit (Cambridge Research Biomedicals, Wilmington, Del.) was used to synthesize the peptides onto derivatized polyethylene pins by the method originally described by Geysen et al. (10). The immobilized

TABLE 1. Summary of antibodies and antisera used

Antibody	Antigen	Specificity(ies)
Polyclonal		
LAH2	*C. coli* VC167-T2 whole cells absorbed against VC167-T1 whole cells (14)	T2 flagellar surface,[a] T2 FlaA flagellin[b]
MEP2	*C. coli* VC167-T2 whole cells (this study)	Non-surface binding, T2 FlaA flagellin
E288	*C. coli* VC167-T2 SDS-denatured flagellin cut from nitrocellulose (this study)	Non-surface binding, T2 FlaA flagellin
M27	*C. coli* VC167-T2 HPLC-purified flagellin (this study)	Non-surface binding, T2 FlaA flagellin
Y29	Fusion of *C. coli* VC167-T2 *flaA* (residues 55 to 337) to protein A in pRIT5 (this study)	T2 FlaA amino acids 55–337, non-surface binding
Y30	*S. dublin* flagella expressing *C. coli* VC167-T2 FlaB residues 261 to 276	T2 FlaB amino acids 261–276, non-surface binding
PG4	Synthetic *C. coli* VC167-T2 FlaA peptide (residues 170 to 182) coupled to BSA synthetic peptide (this study)	T2 FlaA amino acids 170–182, non-surface binding
LINA	*C. coli* VC167-T1 whole cells (14)	Surface binding, T2 FlaA flagellin
SML1	*C. jejuni* VC74 whole cells (23)	Non-surface binding, T2 FlaA flagellin
SML2	*C. jejuni* VC74 SDS-denatured flagellin (23)	Non-surface binding
Monoclonal		
M39	*C. jejuni* VC74 flagellin (23)	Non-surface binding, T2 FlaA flagellin
72c	*H. pylori* flagellin (18)	Non-surface binding, T2 FlaA flagellin

[a] As determined by immunogold electron microscopy with *C. coli* VC167-T2 flagella and by ELISA before and after absorption with live motile *C. coli* VC167-T2 cells.
[b] As determined by Western blot analysis.

peptides were then used to screen for antibody epitopes. Initially the pins were blocked with 2% (wt/vol) BSA–0.2% (wt/vol) Na-caseinate in 10 mM Tris HCl–0.85% (wt/vol) NaCl–0.05% (vol/vol) Tween 20 (Tris-NaCl-Tween) (pH 7.4) for 1 h. Rabbit antiflagellin polyclonal antisera, diluted 1:200 in Tris-NaCl-Tween, or mouse antiflagellin monoclonal antibodies, diluted 1:1,000, were incubated with the peptides overnight at 4°C. The pins were washed three times for 15 min with Tris-NaCl-Tween and incubated with goat anti-rabbit immunoglobulin G (IgG) (Caltag Laboratories, South San Francisco, Calif.) or goat anti-mouse immunoglobulin G (Caltag) conjugated to alkaline phosphatase, depending on the primary antibody type, for 1 h. The pins were washed three times as described above and incubated with alkaline phosphatase substrate solution (1 M ethanolamine, 0.5 mM $MgCl_2$, 3.8 mM *para*-nitrophenyl phosphate, pH 9.5), and the color reaction was developed for 30 min. The A_{405} was read with an EIA model 310 enzyme-linked immunosorbent assay (ELISA) reader (Biotek Instruments Inc., Highland Park, Vt.). The solid-phase peptides were reused according to the manufacturer's instructions.

Immunoblotting and ELISAs. After electrotransfer, reactive sites on the nitrocellulose membrane were blocked with 2% (vol/vol) skim milk in Tris-NaCl for 1 h at room temperature. The nitrocellulose was then incubated with an appropriate dilution of antiserum in Tris-NaCl for 2 h, washed three times in Tris-NaCl, and incubated with either alkaline phosphatase-conjugated goat anti-rabbit or goat anti-mouse antibody (Caltag) diluted 1:3,000 in Tris-NaCl. After incubation for 1 h, the nitrocellulose was washed three times in Tris-NaCl and the immunoreactive bands were visualized with the substrate 5-bromo-4-chloro-3-indoylphosphate (Sigma) and nitroblue tetrazolium (Sigma).

The ELISA was carried out by using a microtiter plate modification of the method of Engvall and Perlmann (6). Briefly, intact flagellar filaments or glycine-extracted flagellin (0.3 μg of protein per well) were incubated in microtiter plate wells overnight. Following blocking with 2% (wt/vol) BSA in Tris-NaCl-Tween (pH 7.4), serial doubling dilutions of antisera were added to the wells and incubated for 1 h. The wells were washed three times with Tris-NaCl-Tween and incubated with a 1:3,000 dilution in Tris-NaCl of either goat anti-rabbit or anti-mouse antibody conjugated to alkaline phosphatase. The wells were washed as described above, and the substrate (*p*-nitrophenyl phosphate; Sigma) was added. The A_{405} was read.

Immunogold electron microscopy. Bacterial cells or sheared flagellar filaments on Formvar-coated grids were incubated with 0.4% (wt/vol) BSA in Tris-NaCl for 30 min and then with a 1:20 dilution of polyclonal antiserum or a 1:100 dilution of monoclonal antibody in 10 mM Tris-HCl for 1 h. The grids were washed three times in 10 mM Tris-HCl and incubated with a 1:50 dilution of protein A-colloidal gold (15 nm) (Jannsen Pharmaceutica, Olen, Belgium). After an additional five washes in Tris-NaCl, the grids were negatively stained with 1% (wt/vol) ammonium molybdate in distilled water (pH 7.0) and examined on a Phillips EM300 microscope at an accelerating voltage of 60 kV.

RESULTS

Molecular weight studies. Because the subunit M_r of *C. coli* VC167-T2 FlaA flagellin estimated by SDS-PAGE analysis (59,500) differs somewhat from that predicted from the nucleotide sequence of the *flaA* gene (58,884) and because post-translational modifications can affect the accuracy of M_r estimation by SDS-PAGE, sedimentation analysis, which is based on a different principle, was used to provide a second estimate of the molecular weight of the protein in solution at pH 2.1. SDS-PAGE analysis confirmed that no breakdown of the flagellin had occurred during the ultracentrifugation run, and the plot of ln y versus r^2 (data not shown) showed limited

upward curvature, indicating that extensive aggregation of flagellin had not occurred under the conditions used. The weight-average molecular weights ranged from 51,000 at the cell top to 74,000 at the cell bottom. The weight-average molecular weight computed across the whole cell was 63,000. This value is significantly different from the 58,884 predicted from the nucleotide sequence and is consistent with the mature protein being posttranslationally modified.

Far-UV CD spectral analysis of secondary structure. The secondary structure of the *C. coli* VC167-T2 FlaA flagellin was determined by CD measurements in the far-UV spectral region. These spectra are presented in Fig. 1, and the data obtained by two methods to measure protein concentration are summarized in Table 2. Under the various assay conditions used, the protein displayed a sizable amount of both β-sheet (35 to 48%) and β-turn (11 to 29%) structure. However, the α-helix content of the protein differed significantly depending on the assay conditions. At pH 2.2, which was employed to dissociate the flagellar filament, or at pH 7.5, the α-helix content was 5 to 9%. When measured in the presence of 0.1% SDS to mimic the hydrophobic environment to which the monomers would be expected to be exposed in the assembled filament, the α-helix content increased to 12 to 16%. In the presence of 50% trifluoroethanol, which also mimics a nonpolar environment, the α-helix content was increased to 18 to 26%. This α-helix content was consistent with the 25.5% α-helix content predicted by the algorithm of Garnier et al. (8). This algorithm also predicts a β-sheet content of 36.3%, again agreeing with the values obtained by CD measurements.

Near-UV CD spectra. Near-UV CD spectra were measured at pH 7.5 and 2.2, using the protein concentration determined by fringe counts. Because the *C. coli* VC167-T2 FlaA flagellin contains no Trp or Cys residues, the CD signal observed in this region arises from composite contributions from some or all of the aromatic residues, which in this case are 9 tyrosines and 18 phenylalanines. A broad negative trough around 280 nm probably arises from the tyrosines (Fig. 1, inset). There is also some additional fine structure apparent from 270 to 250 nm arising from the phenylalanines. The spectrum at pH 2.2 shows a reduced negative ellipticity compared with that at pH 7.5, which is consistent with a looser structure and the slightly reduced α-helix content observed at the acid pH.

Proteolytic characterization. The domain structure of *C. coli* VC167-T2 FlaA flagellin was examined by using controlled proteolysis of purified flagellin with several enzymes with specific cleavage sites. When intact FlaA flagellar filaments were treated with trypsin (Lys or Arg specific), chymotrypsin (Phe, Thr, or Tyr specific), or endoproteinase Glu-C (Asp or Glu specific in phosphate buffer) for 6 h at enzyme-to-protein ratios of 1:50 and 1:200, no flagellin digestion was observed (data not shown). However, when purified FlaA flagellin was incubated at an enzyme-to-flagellin ratio of 1:250, TPCK-treated typsin cleaved the purified flagellin to produce a predominant cleavage peptide with an apparent M_r of 22,000 (Fig. 2A). Automated Edman degradation identified the amino-terminal residue of this trypsin-resistant 22,000-M_r peptide as Phe-173 (Fig. 3A). At the same enzyme-to-flagellin ratio, chymotrypsin cleaved the flagellin to produce a major cleavage peptide with an approximate M_r of 23,000 (Fig. 2B). Automated Edman degradation identified the amino-terminal residue of this chymotrypsin-resistant 23,000-M_r peptide as Asn-193 (Fig. 3A). In the case of endoproteinase Glu-C digestion, the major cleavage peptide had an apparent M_r of 24,000 (Fig. 2C). Sequence analysis identified the amino-terminal residue of this endoproteinase Glu-C-resistant 24,000-M_r peptide as Phe-146 (Fig. 3A).

Epitopic analysis. Mimeotope analysis was used to provide information on the positioning of amino acids in the FlaA sequence with respect to the surface of the assembled flagellar filament. Octapeptides with a four-amino-acid overlap and covering the entire sequence of the T2 FlaA protein were synthesized and used to determine antibody-peptide reactivities by solid-phase ELISA. With the exception of antiserum Y30, all the antibodies used reacted with the wild-type *C. coli* VC167-T2 FlaA flagellin monomer by Western immunoblot (Table 1). Antiserum Y30 reacted only with the *C. coli* VC167-T2 FlaB flagellin and not with the FlaA flagellin (Table 1). Immunogold electron microscopy and ELISA before and after absorption with the native flagellar filaments on live motile cells of *C. coli* VC167-T2 were used to determine the presence of antibodies to surface-located epitopes. Antisera LAH2 and LINA were the only antisera which contained antibodies to active surface-located epitopes, as shown by the loss of immunogold and ELISA reactivities upon absorption (Fig. 4A and B; Table 1). Polyclonal antiserum Y29, raised against the fusion protein expressing amino acids 54 to 335 of *C. coli* VC167-T2 FlaA, was representative of the remaining antisera and antibodies as demonstrated by the absence of decoration with gold particles on the surface of the flagellar filaments and the low ELISA titer to intact filaments, both of which were unaffected by absorption (Fig. 4C; Table 1).

The accuracy of the mimeotope technique was illustrated by the ability of antiserum PG4, which was raised against the synthetic dodecameric peptide ^{170}VTRFETGSQSFSSG^{183}, to react strongly (A_{405} > 0.9) with the mimeotope peptide ^{173}FETGSQSF^{180} (Fig. 3B). Similarly, antiserum Y30, raised against the *Salmonella* flagellin fusion expressing the *Campylobacter* FlaB flagellin ^{261}QINYNDGDNNGQLIS^{275} peptide, reacted only with mimeotope peptide ^{263}NYNDGDNNGQLI^{274} (Fig. 3B) (A_{405} = 1.9). This reaction was clearly specific for the FlaB flagellin because the corresponding FlaA sequence is ^{261}KVDYSDGDENGSLIS^{275}. While it is possible that the epitopes recognized by both of these antisera were present on the surface of the flagellar filament in an inactive conformation, it is most likely that they were masked in the assembled wild-type VC167-T2 flagellar filament. The second epitope, ^{263}NYNDGDNNGQLI^{274}, was also apparently buried in the truncated FlaB filament produced by a *flaA flaB*$^+$ mutant.

The use of the various other non-surface-reactive antisera and antibodies allowed identification of other apparently non-surface-exposed residues in the FlaA sequence. Figure 3B and D show that six groups of these putative nonexposed residues were distributed along the length of the linear map of FlaA flagellin. The first major cluster (cluster I) was shown with antiserum E288, raised against SDS-denatured *C. coli* VC167-T2 flagellin, which displayed strong reactivity with the N-terminal 92 residues. Also in this first cluster was ^{89}DTIK TKAT^{96}, which was a major epitope recognized by antiserum SML2 (A_{405} = 0.6), another antiserum raised against heterologous SDS-denatured *Campylobacter* flagellin. Overlapping this epitope was the major epitope (A_{405} > 0.7) recognized by antiserum Y29, ^{85}LKILDTIK^{92}. This overlapping sequence appears to be conserved in the *Campylobacter* flagellins sequenced to date. Cluster II was contained between residues 129 and 188 and included the previously described PG4 epitope. Epitopes contained in cluster III were between residues 225 and 337 and in the case of FlaB would include the FlaB-specific epitope described above as well as ^{237}SVG AYAIK^{244}, recognized by antiserum SML2 (A_{405} = 0.6), ^{245}AGNTSQDF^{252}, recognized by monoclonal antibody M39, and ^{317}GILHTENY^{324} and ^{329}LVKNDGRD^{336}, recognized by antisera Y29 and E288, respectively (A_{405} > 0.35). Cluster IV

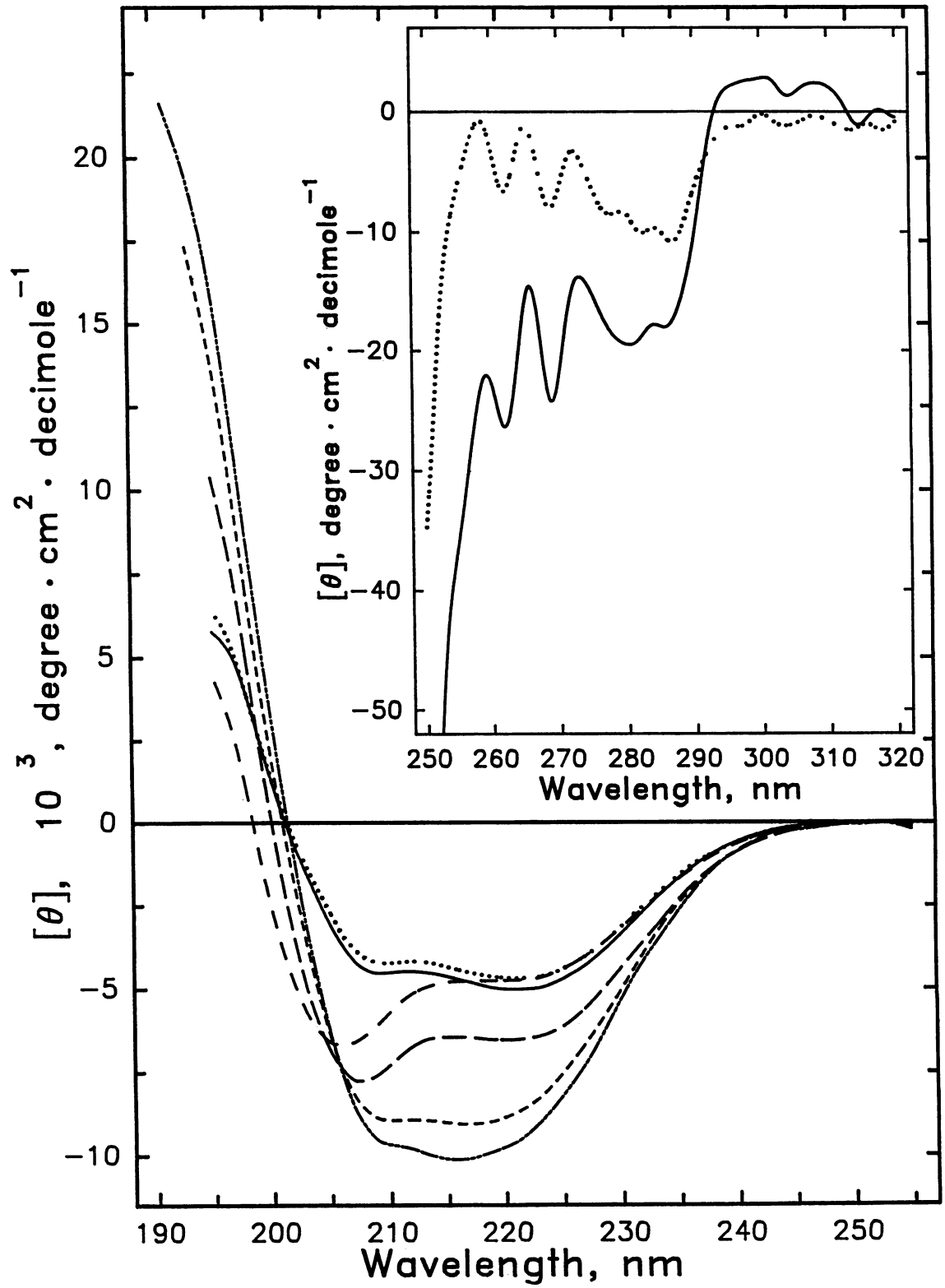

FIG. 1. UV spectral analysis of *C. coli* VC167-T2 FlaA flagellin. Far-UV CD spectra. The protein concentration was 0.989 mg/ml, and the solvent systems were 0.145 M NaCl–20 mM Tris HCl (pH 7.5) (———), 0.1% SDS (pH 7.5) (– – –), 200 mM glycine (pH 2.2) (· · ·), 0.1% SDS (pH 2.2) (— — —), 50% (vol/vol) trifluoroethanol (pH 7.5) (- - -), and 50% (vol/vol) trifluoroethanol (pH 2.2) (— · ·). (Inset) Near-UV spectra of flagellin in 0.02 M Tris–0.145 M NaCl (pH 7.5) (———) and in 0.2 M glycine (pH 2.2) (· · ·). The protein concentration was 1.08 mg/ml.

TABLE 2. Secondary structure of the FlaA flagellin of *C. coli* VC167-T2 from analysis of solution CD spectra by the Provencher-Glöckner program

Solvent	Protein estimate[a]	Secondary structure content (%)			
		α-Helix	β-Sheet	β-Turn	Remainder
145 mM NaCl–20 mM Tris HCl (pH 7.5)	FC	9	41	23	27
(pH 7.5 solvent)	CE	12	39	21	28
pH 7.5 solvent + 0.1% SDS	FC	12	42	21	25
	CE	15	41	19	26
0.2 M glycine (pH 2.2)	FC	5	42	29	24
	CE	10	35	22	27
pH 2.2 glycine + 0.1% SDS	FC	16	38	24	22
	CE	21	45	21	23
pH 7.5 solvent + 50% TFE	FC	21	48	22	10
	CE	26	45	18	11
pH 2.2 glycine + 50% TFE	FC	18	43	16	23
	CE	22	38	11	28

[a] Protein concentration estimated by fringe counts (FC) or from calculated extinction (CE) values.

stretched from residue 389 to 428, including ^{421}YSAILSAS^{428}, which reacted strongly with monoclonal antibody M39. Cluster V, starting at residue 461, contained only four epitopes, including another apparently conserved epitope recognized by the heterologous antiserum SML2, ^{497}DQIRADIG^{504}. Cluster VI stretched from residue 533 to 560 and included a second epitope which reacted strongly with monoclonal antibody M39, ^{541}ANYSKANI^{548}.

In an effort to identify immunoaccessible peptides present on the surface of the native flagellar filament, including LAH2-serospecific sequence, the two surface-reactive polyclonal antisera LAH2 and LINA were also tested. However, the results in Fig. 3C show that very few of the linear peptides were reactive with either antiserum. Absorption of these antisera against intact native VC167-T2 flagellar filaments did not alter the ELISA reactivities of these peptides, indicating that these residues were not exposed in an active form on the surface of the native flagellar filament.

Localization of serotypic domain. The LAH2 immunoreactivity of T2 FlaA flagellin was lost upon digestion with trypsin, chymotrypsin, or endoproteinase Glu-C (data not shown); however, controlled proteolysis with the Lys-specific endoproteinase Lys-C allowed the localization of the LAH2-serospecific domain of the T2 FlaA flagellin. Digestion of T2 FlaA at an enzyme-to-protein ratio of 1:100 for 18 h resulted in an endoproteinase Lys-C-resistant peptide with an apparent M_r of 35,000, together with a number of other minor digestion products with lower M_rs (Fig. 5, lane 2). Automated Edman degration showed that the amino-terminal residue of this 35,000-M_r peptide was Ala-245, and Western blot analysis showed that this peptide was reactive with the T2 FlaA-specific antiserum LAH2 (Fig. 5, lane 3). Several of the less predominant peptides with lower molecular weights were also reactive with this antiserum, with the smallest migrating with an apparent M_r of 20,000 (Fig. 5, lane 3). Sequence analysis showed that this peptide possessed the same amino-terminal sequence as the immunoreactive peptide with an apparent M_r of 35,000 (Fig. 3A).

Further information on the location of the LAH2-serospecific domain was obtained by digestion with endoproteinase Arg-C. Although *C. coli* VC167-T2 FlaA flagellin was resistant to digestion with this enzyme and the majority of flagellin remained uncut after treatment at an enzyme-to-protein ratio of 1:50 for 9 h, two minor peptides which ran as a doublet with apparent M_rs of 29,000 and 28,000 and which were strongly reactive with LAH2 antiserum in Western immunoblot assays were produced (data not shown). Automated Edman degradation showed that the amino-terminal residue of the 29,000-M_r peptide was Lys-366, while that of the 28,000-M_r peptide was Phe-379 (Fig. 3A).

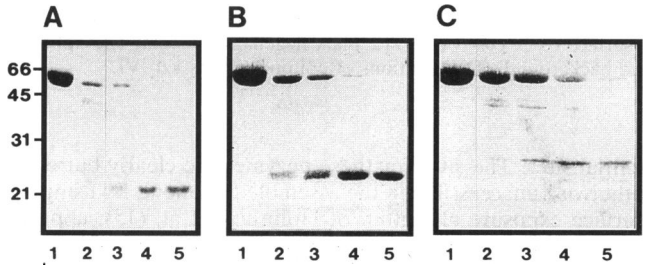

FIG. 2. Coomassie blue-stained SDS-PAGE gels of limited proteolysis of *C. coli* VC167-T2 flagellin with trypsin (enzyme/protein ratio, 1:250) (A), chymotrypsin (1:250) (B), and endoproteinase Glu-C (1:200) (C). Lanes 1, flagellin at time zero; lanes 2, 5 min; lanes 3, 30 min; lanes 4, 1 h; and lanes 5, 6 h. Molecular weight markers (10^3) are indicated on the left.

DISCUSSION

This study has provided new information on the molecular weight and secondary and domain structures of the predominant flagellin species in *Campylobacter* flagella and on the folding of the FlaA subunit as it exists in the assembled flagellar filament. With a solution weight-average molecular weight of 63,000, the FlaA flagellin of *C. coli* VC167-T2 is among the largest of the procaryotic flagellins characterized to date (42). Comparison with the 58,884 M_r deduced from the *flaA* gene sequence and the 59,500 M_r estimated by SDS-PAGE indicates that posttranslational modification possibly

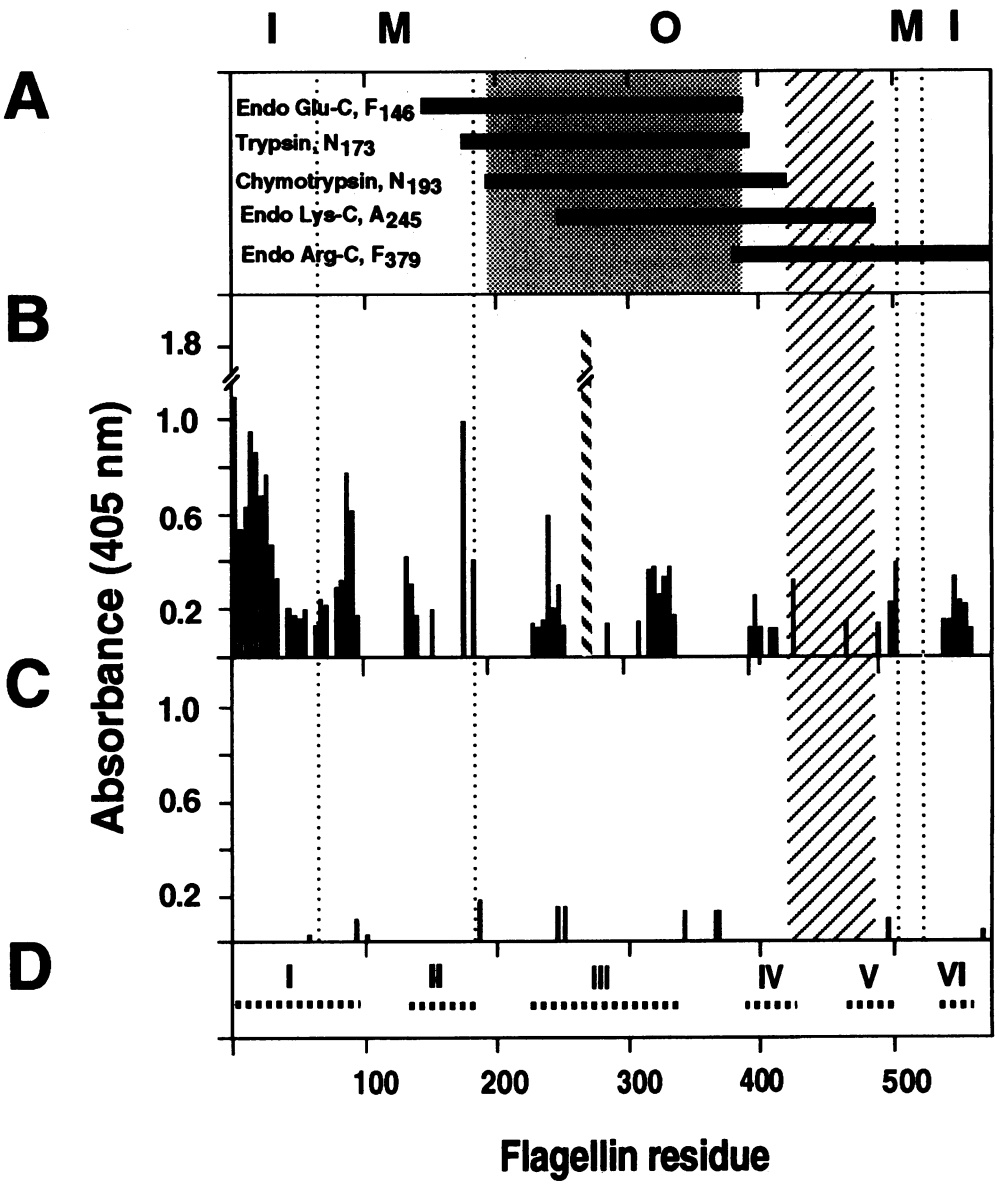

FIG. 3. (A) Positions of isolated protease fragments relative to the linear map of *C. coli* VC167-T2 FlaA flagellin. The number of the N-terminal residue determined by automated Edman degradation is indicated, the major protease-resistant domain is shaded, and the apparent position of the LAH2-serospecific domain is shown by the cross-hatched background. The segments corresponding to the inner (I), middle (M), and outer (O) domains of *Salmonella* flagellin are also indicated, on the basis of sequence comparison (16, 38). (B) Mimeotope analysis of FlaA octapeptide reactivity (A_{405}) with antibodies unable to bind to the surface of *C. coli* VC167-T2 FlaA flagellar filaments. The cross-hatched epitopic reactivity is that of FlaB-specific antiserum Y30 with FlaB-specific peptide ^{263}NYNDGDNNGQLI^{274}. The apparent position of the LAH2-serospecific domain is also shown by the cross-hatched background. (C) Mimeotope analysis of FlaA octapeptide reactivity (A_{405}) with polyclonal antisera LAH2 and LINA, which contained antibodies able to bind to the surface of *C. coli* VC167-T2 FlaA flagellar filaments. The apparent position of the LAH2-serospecific domain is also shown by the cross-hatched background. (D) Locations of epitope groups I to VI.

accounts for approximately 1,000 to 3,000 of the M_r of this flagellin. Together with the lesser FlaB species, this 572-residue FlaA flagellin is folded and assembled into a flagellar filament which exposes some or all of the posttranslational modification on the filament surface to provide serospecificity for LAH2 antiserum. The folding and assembly process provides a filament which is resistant to digestion by proteases such as trypsin, which has 45 potential cleavage sites in the primary structure of FlaA flagellin, chymotrypsin, which has 27 potential sites, and endoproteinase Glu-C, which has 48 potential sites. The sites for these enzymes are clearly buried or otherwise unaccessible in the assembled filament. By using the surface exposure algorithm of Holbrook et al. (15), approximately 290 of the FlaA residues are predicted to be buried in the monomer. Indeed, the mimeotope analysis undertaken in this study together with the ELISA and immunogold electron microscopy analyses indicate that that as many as 416 residues or 72.7% of the residues may be nonaccessible when the flagellin monomers are assembled into the flagellar filament. However, because of the possibility that certain epitopes may

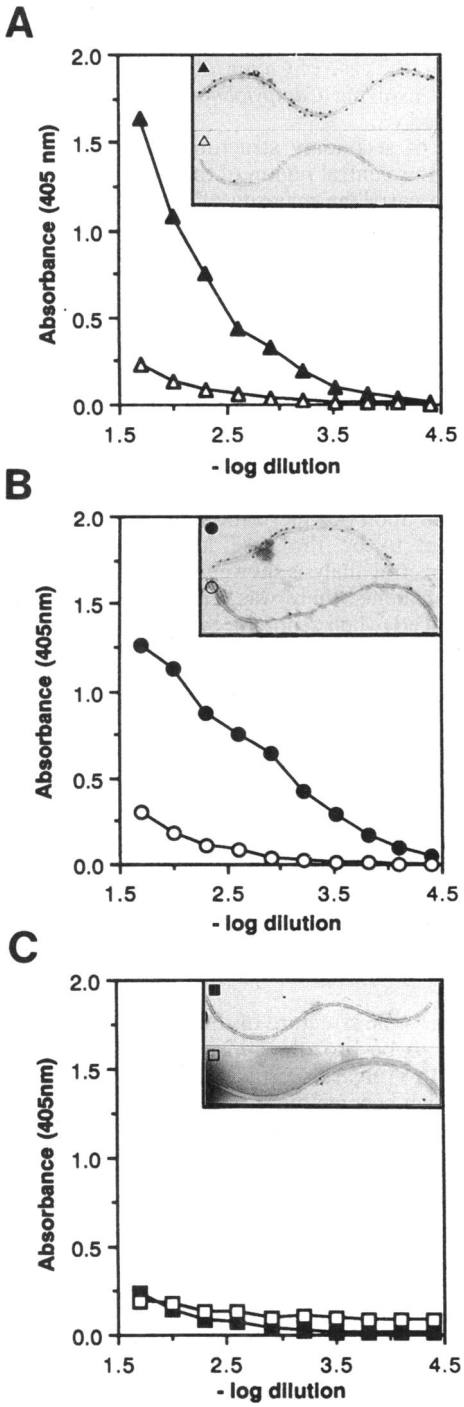

FIG. 4. Analysis of the ability of antibodies to bind to the surface of *C. coli* VC167-T2 FlaA flagellar filaments as determined by immunogold electron microscopy (insets) and ELISA of FlaA flagellin before (▲, ●, ■) and after (△, ○, □) absorption of antisera LAH2 (A), LINA (B), and Y29 (C) with the native flagellar filaments on live motile cells of *C. coli* VC167-T2.

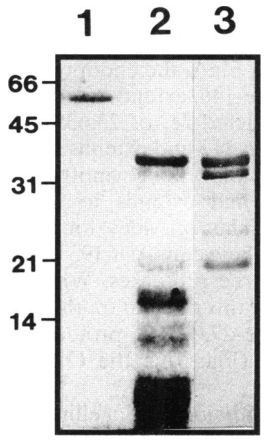

FIG. 5. SDS-PAGE of undigested flagellin of *C. coli* VC167-T2 (lane 1) and flagellin digested for 18 h with endoproteinase Lys-C at a protein-to-enzyme ratio of 100:1 (lane 2). Lane 3 is the digested material from lane 2 Western immunoblotted with antiserum LAH2 at a dilution of 1:5,000. Molecular weight markers (10^3) are indicated on the left.

be on the surface of the filament but locked in an inactive conformation, some caution needs to be taken with this prediction.

With a length of 572 residues, the *C. coli* VC167-T2 FlaA flagellin is longer than the *Enterobacteriaceae* flagellins whose sequences have been predicted from DNA sequence analysis (42). For example, it is 78 residues larger than the *Salmonella typhimurium* serotype *i* flagellin (16). Despite this difference in length, the *Campylobacter* and *Salmonella* flagellins have considerable sequence similarity. Under conditions of optimum alignment and on the basis of the *Campylobacter* sequence length, the two flagellin species have 41.8% sequence identity. However, in addition to the difference in the lengths of the two flagellin species, which in and of itself will contribute to differences in higher-order structure, there are significant differences in the primary sequences, which will also influence higher-order structure. For example the *Salmonella* protein has five α-helix-breaking proline residues which are lacking in the *Campylobacter* molecule. There are also differences in the relative content and positioning of Tyr and Phe residues, which presumably account for the quite different near-UV spectra of the *Salmonella* and *Campylobacter* flagellins. The dominant features of the *Salmonella* protein are a large positive peak centered at 290 nm and another, smaller one at 280 nm (38). The near-UV region from 250 to 300 nm depends on the environment and clustering of the aromatic side chains, which makes it a sensitive tool for detecting both differences and changes in tertiary structure. Because neither of the *Salmonella* spectral features is present in the case of the *Campylobacter* flagellin, the two flagellins appear to display different tertiary structures.

Another difference, albeit subtle, appears to be in the domain structure of *Campylobacter* flagellin as revealed by protease digestion studies. Studies by Vonderviszt et al. (39) have shown that digestion of *Salmonella* flagellin with trypsin or subtilisin results in an intermediate peptide with an M_r of 40,000 followed by a stable protease-resistant peptide with an M_r of 27,000. In the case of *C. coli* VC167-T2 flagellin, a stable protease-resistant domain was obtained with trypsin, chymotrypsin, and endoproteinase Glu-C, but there was little evidence of an intermediate, so-called less-exposed or middle domain. For all three proteases, any intermediate peptides formed were quite transient, and most of the degraded protein appeared as stable enzyme-resistant peptides with approximate M_rs ranging from 21,000 to 24,000. These three enzyme-resistant peptides were overlapping (Fig. 3A). While we have

been unable to determine the carboxy-terminal residues of any of the peptides generated in the study, on the basis of the deduced sequence of FlaA, the endoproteinase GluC-resistant peptide begins at Phe-146, extends to Asp-375, and produces a peptide with a predicted M_r of 23,635. The trypsin-resistant peptide begins at Asn-173 and extends to Lys-388 to produce a 22,000-M_r peptide, and the chymotrypsin-resistant peptide begins at Asn-193 and extends to Tyr-421 to produce a 23,000-M_r peptide. This provides for a domain of approximately 187,000 M_r between Asn-193 and Asp-375 which is resistant to these three proteases. While the position of the N-terminal region of this domain on the linear flagellin map is similar to that of the 27,000-M_r protease resistant domain of *Salmonella* flagellin (Fig. 3A), the *Campylobacter* domain is considerably smaller.

In the case of the *Salmonella* flagellin, the protease-resistant domain has been shown to lie within the D3 structural domain, which corresponds to the outward-facing globular domain of the filament in electron density maps (25). This domain also contains sequence that is highly variable among the enterobacterial flagellins. However, in the cases of *Campylobacter* spp. and two other members of the *Proteobacteria* subdivision *Thiovulum-Campylobacter* (20), *Wolinella succinogenes* and *H. pylori*, there are two conserved sequence boxes contained within this protease-resistant domain (35). Schuster et al. (35) have recently suggested that these two conserved regions may have a structural role, possibly being responsible for the shape of the flagellar filament formed by this group of bacteria, which show flagellar surface patterns of parallel lines along the axis of their filament. Interestingly, in the current study, none of the antibodies employed in the mimeotope analysis were found to bind to linear peptides comprising either of the two conserved sequence boxes. Indeed, in the case of *Campylobacter* FlaA flagellin, the trypsin-chymotrypsin-, and endoproteinase Glu-C-resistant peptides also did not react in Western blots with antiserum LAH2, which bound to the flagellar surface. However, digestion with endoproteinase Lys-C and endoproteinase Arg-C showed that a segment of sequence C terminal to the trypsin-chymotrypsin-endoproteinase Glu-C-resistant domain carried LAH2-reactive sequence. A minor endoproteinase Arg-C cleavage peptide which begins at Phe-379 and extends to the C-terminal residue of FlaA was reactive with antiserum LAH2. Cleavage with endoproteinase Lys-C also yielded a minor peptide with an apparent M_r of 20,000 by SDS-PAGE beginning at Ala-245 which was reactive with LAH2 antiserum. Comparison with the deduced FlaA sequence suggests that the SDS-PAGE estimate is inaccurate and that the most likely cleavage site is after Lys-480, which would provide a modified peptide with a deduced M_r of 234,000. Taken together, these data position the LAH2-reactive sequence between residues 421 and 480 (Fig. 3B). In this regard, earlier studies have shown that several serine residues in the region from positions 422 to 451 are posttranslationally modified (23). Neither the chemical nature of the serine modification nor the contribution of the modification to LAH2 reactivity has been identified; however, it is likely that the modified serines contribute to the apparent aberrant electrophoretic migration of the LAH2-reactive endoproteinase Lys-C peptide. Examination of the FlaA sequence also shows direct repeats GSGFSAGSG beginning at residues 404 and 447, which includes some of the modified serines. The repeats are encoded by two 27-bp repeats with only three mismatches. In *Salmonella typhi* H1-*d* flagellin, intragenic recombination involving a similar pair of 11-bp repeats in the middle of the *fla* gene can lead to the excision of 261 bp of the *fla* gene (7). In this case the recombination event results in a loss of the *d* serotype and the appearance of a new flagellin serotype, H1-*j*. While there is no evidence that such a mechanism contributes to antigenic differences in the case of *Campylobacter* flagellins, recombination events involving *Campylobacter fla* genes have recently been reported (3).

In terms of secondary structure, by use of a number of algorithms, this central region of the *Campylobacter* flagellin is predicted to carry the majority of the β-sheet content of the molecule. For example, by the algorithm of Garnier et al. (8), 72% of the β-sheet structure is predicted to lie between residues 134 and 462 of the 572-residue FlaA flagellin. This algorithm also predicts that the majority of the α-helical structure is in the terminal regions of the molecule, with 46.6% of the helix in the first 130 residues and 30.1% in the last 100 residues. Algorithms with higher predictive accuracy, such as the recently reported PHD program, make similar predictions with respect to the distribution of helix (34). In the case of the flagellins of the enteric bacteria, these terminal α-helices are thought to be unstable when the protein is free in solution and are stabilized upon polymerization into the filament (37). This also appears to be the case in *Campylobacter* flagellins. Near-UV spectral analysis showed that under conditions which dissociate filaments, there was a looser structure as well as a slightly reduced α-helix content. Similarly, secondary structure analysis showed that there was a sizable increase in α-helix content when hydrophobic and nonpolar conditions were used to mimic conditions in an assembled filament. The amino- and carboxy-terminal regions were also readily digested by proteases when in a soluble monomeric form but were resistant to equivalent or higher concentrations of enzyme in the intact filament. Finally, mimeotope analysis suggested that the 92 amino-terminal residues were buried in the case of assembled flagella, as were residues 541 to 548 at the carboxy-terminal end of the flagellin molecule. Indeed, immunochemical analysis with antiserum Y29 provided evidence that the non-surface-accessible region at the amino-terminal end of FlaA stretched well into the protease-resistant domain, as far as residue 337.

In summary, the structure of the *Campylobacter* FlaA flagellin appears to be broadly similar to that of enterobacterial flagellin, with protease-sensitive amino- and carboxy-terminal domains which become buried when the flagellin is assembled into the flagellar filament. Between these domains is a centrally located segment of sequence with a protease-resistant domain which is smaller than the equivalent domain in *Salmonella* flagella. Surface-exposed linear epitopic sequence in the molecule could not be identified with polyclonal antisera containing antibodies to epitopes on the flagellar surface, suggesting that a number of the surface-exposed epitopes of *Campylobacter* flagella may be conformation dependent. A segment of surface-exposed sequence which contributes to the serospecificity of the flagellar filament was, however, localized to residues between 421 and 480 following the protease-resistant domain. This region of sequence has previously been shown to contain posttranslationally modified residues (24), and genetic studies have shown that the serospecificity of this flagellin is the result of posttranslational modification (1). The chemical nature of this serospecific posttranslational modification is currently under investigation.

ACKNOWLEDGMENTS

This work was supported in part by grants to T.J.T. from the Medical Research Council of Canada, to P.G. from the U.S. Navy Research and Development Command Research Work Unit (no. 61102A3M 161102BS13 AK.111.), and to C.M.K. from the Medical Research

Council of Canada and the Alberta Heritage Foundation for Medical Research.

We thank Phillip Schellenberg, Richard Alm, and Donald Burr for their contributions to this study.

REFERENCES

1. **Alm, R. A., P. Guerry, M. E. Power, and T. J. Trust.** 1992. Variation in antigenicity and molecular weight of *Campylobacter coli* VC167 flagellin in different genetic backgrounds. J. Bacteriol. **174:**4230–4238.
2. **Alm, R. A., P. Guerry, and T. J. Trust.** 1993. The *Campylobacter* σ^{54} *flaB* flagellin promoter is subject to environmental regulation. J. Bacteriol. **175:**4448–4455.
3. **Alm, R. A., P. Guerry, and T. J. Trust.** 1993. Significance of duplicated flagellin genes in *Campylobacter*. J. Mol. Biol. **230:**359–363.
4. **Babul, J., and E. Stellwagen.** 1969. Measurement of protein concentration with interference optics. Anal. Biochem. **28:**216–221.
5. **Chervenka, C. H.** 1969. A manual of methods for the analytical ultracentrifuge. Spinco Division of Beckman Instruments Inc., Palo Alto, Calif.
6. **Engvall, E., and P. Perlmann.** 1972. Enzyme-linked immunoabsorbent assay, ELISA. III. Quantitation of specific antibodies by enzyme-labelled anti-immunoglobulin in antigen coated tubes. J. Immunol. **109:**128–135.
7. **Frankel, G., S. M. C. Newton, G. K. Schoolnik, and B. A. D. Stocker.** 1989. Intragenic recombination in a flagellin gene—characterization of the H1-j gene of *Salmonella typhi*. EMBO J. **8:**3149–3152.
8. **Garnier, J., D. J. Osguthorpe, and B. Robson.** 1978. Analysis of the accuracy and implications of simple methods for predicting the secondary structure of globular proteins. J. Mol. Biol. **120:**97–120.
9. **Gerl, L., and M. Sumper.** 1988. Halobacterial flagellins are encoded by a multigene family. J. Biol. Chem. **263:**13246–13251.
10. **Geysen, H. M., S. J. Rodda, T. J. Mason, G. Tribbick, and P. G. Scoofs.** 1987. Strategies for epitope analysis using peptide synthesis. J. Immunol. Methods **102:**259–274.
11. **Guerry, P., R. A. Alm, M. E. Power, S. M. Logan, and T. J. Trust.** 1991. Role of two flagellin genes in *Campylobacter* motility. J. Bacteriol. **173:**4757–4764.
12. **Guerry, P., R. A. Alm, M. E. Power, and T. J. Trust.** 1992. Molecular and structural analysis of *Campylobacter* flagellin, p. 267–281. *In* I. Nachamkin, M. J. Blaser, and L. S. Tompkins (ed.), *Campylobacter jejuni*: current status and future trends. American Society for Microbiology, Washington, D.C.
13. **Guerry, P., S. M. Logan, S. Thornton, and T. J. Trust.** 1990. Genomic organization and expression of *Campylobacter* flagellin genes. J. Bacteriol. **172:**1853–1860.
14. **Harris, L. A., S. M. Logan, P. Guerry, and T. J. Trust.** 1987. Antigenic variation of *Campylobacter* flagella. J. Bacteriol. **169:**5066–5071.
15. **Holbrook, S. R., S. M. Muskal, and S. H. Kim.** 1990. Predicting surface exposure of amino acids from protein sequence. Protein Eng. **3:**659–665.
16. **Hyman, H. C., and S. Trachtenberg.** 1991. Point mutations that lock *Salmonella typhimurium* flagellar filaments in the straight right-handed and left-handed forms and their relation to filament superhelicity. J. Mol. Biol. **220:**79–88.
17. **Kalmokoff, M. L., and K. F. Jarrell.** 1991. Cloning and sequencing of a multigene family encoding the flagellins of *Methanococcus voltae*. J. Bacteriol. **173:**7113–7125.
18. **Kostrzynska, M., J. D. Betts, J. W. Austin, and T. J. Trust.** 1991. Identification, characterization, and spatial localization of two flagellin species in *Helicobacter pylori* flagella. J. Bacteriol. **173:**937–946.
19. **Laemmli, U. K.** 1970. Cleavage of structural proteins during the assembly of the head of bacteriophage T4. Nature (London) **227:**680–685.
20. **Lane, D. J., A. P. Harrison, D. Stahl, B. Pace, S. J. Giovannoni, G. J. Olsen, and N. R. Pace.** 1992. Evolutionary relationships among sulfur- and iron-oxidizing eubacteria. J. Bacteriol. **174:**269–278.
21. **LeGendre, N., and P. Matsudaira.** 1988. Direct protein microsequencing from Immobilon-P transfer membrane. BioTechniques **6:**154–159.
22. **Logan, S. M., P. Guerry, D. M. Rollins, D. H. Burr, and T. J. Trust.** 1989. In vivo antigenic variation of *Campylobacter* flagellin. Infect. Immun. **57:**2583–2585.
23. **Logan, S. M., and T. J. Trust.** 1986. Location of epitopes on *Campylobacter jejuni* flagella. J. Bacteriol. **168:**739–745.
24. **Logan, S. M., T. J. Trust, and P. Guerry.** 1989. *Campylobacter* flagellin: evidence for posttranslational modification and gene duplication. J. Bacteriol. **171:**3031–3038.
25. **Namba, K., I. Yamashita, and F. Vonderviszt.** 1989. Structure of the core and central channel of bacterial flagella. Nature (London) **342:**648–654.
26. **Newton, S. M. C., C. O. Jacob, and B. A. D. Stocker.** 1989. Immune response to cholera toxin epitope inserted in *Salmonella* flagella. Science **244:**70–72.
27. **Nuijten, P. J. M., A. J. A. M. V. Asten, W. Gaastra,and B. A. M. van der Zeijst.** 1990. Structural and functional analysis of two *Campylobacter jejuni* flagellin genes. J. Biol. Chem. **265:**17798–17804.
28. **Pallesen, L., and P. Hindersson.** 1989. Cloning and sequencing of a *Treponema pallidum* gene encoding a 31.3-kilodalton endoflagellar subunit (FlaB2). Infect. Immun. **57:**2166–2172.
29. **Parales, J. J., and E. P. Greenberg.** 1991. N-terminal amino acid sequences and amino acid compositions of the *Spirochaeta aurantia* flagellar filament polypeptides. J. Bacteriol. **173:**1357–1359.
30. **Pavlovskis, O. R., D. M. Rollins, R. L. Haberberger, A. E. Green, L. Habash, S. Strocko, and R. I. Walker.** 1991. Significance of flagella in colonization resistance of rabbits immunized with *Campylobacter* spp. Infect. Immun. **59:**2259–2264.
31. **Pleier, E., and R. Schmitt.** 1991. Expression of two *Rhizobium meliloti* flagellin genes and their contribution to the complex filament structure. J. Bacteriol. **173:**2077–2085.
32. **Power, M. E., R. A. Alm, and T. J. Trust.** 1992. Biochemical and antigenic properties of the *Campylobacter* flagellar hook protein. J. Bacteriol. **174:**3874–3883.
33. **Provencher, S. W., and J. Glöckner.** 1981. Estimation of globular protein secondary structure from circular dichroism. Biochemistry **20:**33–37.
34. **Rost, B., and C. Sander.** 1993. Prediction of protein structure at better than 70% accuracy. J. Mol. Biol. **232:**584–599.
35. **Schuster, S. C., M. Bauer, J. Kellermann, F. Lottspeich, and E. Baeuerlein.** Nucleotide sequence of *Wolinella succinogenes* flagellin, which contains in the antigenic domain two conserved regions also present in *Campylobacter* spp. and *Helicobacter pylori*. Submitted for publication.
36. **Towbin, H., T. Staehelin, and J. Gordon.** 1979. Electrophoretic transfer of proteins from polyacrylamide gels to nitrocellulose sheets: procedure and some applications. Proc. Natl. Acad. Sci. USA **74:**4350–4354.
37. **Vonderviszt, F., S. Aizawa, and K. Namba.** 1991. Role of the disordered terminal regions of flagellin in filament formation and stability. J. Mol. Biol. **221:**1461–1474.
38. **Vonderviszt, F., S. Kanto, S. Aizawa, and K. Namba.** 1989. Terminal regions of flagellin are disordered in solution. J. Mol. Biol. **209:**127–133.
39. **Vonderviszt, F., H. Ueadaira, S. I. Kidokoro, and K. Namba.** 1990. Structural organization of flagellin. J. Mol. Biol. **214:**97–104.
40. **Wei, L.-N., and T. M. Joys.** 1985. Covalent structure of three phase-1 flagellar filament proteins of *Salmonella*. J. Mol. Biol. **186:**791–803.
41. **Weissborn, A., H. M. Steinman, and L. Shapiro.** 1982. Characterization of the proteins of the *Caulobacter crescentus* flagellar filament. J. Biol. Chem. **257:**2066–2074.
42. **Wilson, D., and T. J. Beveridge.** 1993. Bacterial flagella filaments and their component flagellins. Can. J. Microbiol. **39:**451–472.
43. **Wu, J. Y., S. Newton, A. Judd, B. Stocker, and W. S. Robinson.** 1989. Expression of immunogenic epitopes of hepatitis B surface antigen with hybrid flagellin proteins by a vaccine strain of *Salmonella*. Proc. Natl. Acad. Sci. USA **86:**4726–4730.